

# Ground Motions and Site Effects from the 2011, M9.0 Tohoku, Japan Earthquake



**H. Ghofrani**

*Department of Earth Sciences, Western University, Canada*

**K. Goda**

*Civil Engineering Department, University of Bristol, UK*

**G.M. Atkinson**

*Department of Earth Sciences, Western University, Canada*

## **SUMMARY:**

Site response is characterized using hundreds of surface and borehole recordings from the 2011 M9.0 Tohoku earthquake and other Japanese events. Site effects were strong at high frequencies for the Tohoku event, despite the expectation that high-frequency response may be damped by nonlinear effects. Using spectral ratios of weak to strong ground motions, localized nonlinearity is inferred for some sites during the Tohoku event, but it was not pervasive. We develop models relating horizontal-to-vertical spectral ratios as a preliminary measure of site amplification to physical characteristics of sites. Finally, we compare site-corrected ground motion observations to predictions obtained from generic ground-motion equations for a reference condition, for the Tohoku mainshock. There is general agreement between observations and predictions for at least some of the published ground-motion prediction equations (GMPEs) for interface events; however, the site corrections involved were much larger than typical “NEHRP factors” as applied in most building codes.

*Keywords: Site effect, cross-spectral ratios, nonlinearity, horizontal-to-vertical spectral ratios, GMPE*

## **1. INTRODUCTION**

Site amplification, or the increase in amplitudes of seismic waves as they traverse soft soil layers near the Earth’s surface, is a major factor influencing the extent of earthquake damage to structures (Field and Jacob, 1995). Understanding of site-specific amplification effects and their role in determining ground motions is important for the design of engineered structures.

We perform an extensive analysis of site amplification during the 2011 Tohoku event by taking advantage of surface and borehole motions from the KiK-net (KIBAN kyoshin network: <http://www.kik.bosai.go.jp/>) to estimate the site transfer functions for all KiK-net stations. Furthermore, detailed assessment of both linear and nonlinear site effects is conducted by investigating changes of site responses in amplitudes as well as fundamental frequency which is defined as the peak of the horizontal-to-vertical (H/V) spectral ratios of the recorded strong motions at the sites (Lermo and Chávez-García, 1993; Theodulidis and Bard, 1995; Fukushima et al., 2007). The applicability of the H/V spectral ratio technique as an alternative tool to estimate site response is evaluated by modeling a relationship between H/V ratios and surface-to-borehole spectral ratio (S/B) ratios, as a function of physical site properties, such as  $V_{S30}$ ,  $f_0$ , and depth-to-bedrock. We develop a suite of simple, useful, and reliable models for prediction of site amplification effects based on available site parameters. Finally, we develop an empirical model of ground motions from the Tohoku earthquake (including site effects) and compare it to the predictions of several ground motion prediction equations (GMPEs) commonly used in seismic hazard analysis applications.

## 2. STRONG GROUND MOTION DATA AND RECORD PROCESSING

The strong-motion data used in this study were collected from the KiK-net. KiK-net consists of 687 strong-motion observation stations installed both on the ground surface and at the bottom of boreholes. We supplement the Tohoku-event data by adding all other events of  $M \geq 5.5$  that were recorded at the KiK-net stations from 1998 to 2009. For all KiK-net stations, 30453 records from 258 earthquakes were processed and analyzed. The number of events for each station varies from 4 to 150. The processing procedure includes windowing, correction for baseline trends, and band-pass filtering. We have applied non-causal, band-pass Butterworth filters with an order of 4. The selected frequency range of analysis is 0.1 to 15 Hz.

## 3. SITE RESPONSE USING SURFACE-TO-BOREHOLE SPECTRAL RATIO (S/B)

In this study, we use an alternative to the standard spectral ratio (SSR) method (Borcherdt, 1970), called the surface-to-borehole spectral ratio (S/B) approach, where the reference site is at the bottom of a borehole directly below the soil site, rather than at a bedrock surface away from the site. S/B spectral ratios are used to provide a direct measure of site response. However, destructive interference between the up-going incident wave field and down-going reflected waves from the surface at specific frequencies can produce a notch in the (Fourier Amplitude Spectrum) FAS of the borehole recording (Steidl et al., 1996). The surface-to-borehole ratios corrected for the depth effect,  $S/B'$ , can be obtained by multiplying S/B by the coherence ( $C^2$ ) between surface and borehole recordings (Steidl et al., 1996):

$$S/B' = C^2(S/B) \quad (1)$$

where

$$C^2 = \frac{|S_{12}(f)|^2}{S_{11}(f)S_{22}(f)} \quad (2)$$

in which  $S_{11}(f)$  and  $S_{22}(f)$  are the power spectral densities of the accelerograms recorded at the surface and downhole, respectively, and  $S_{12}(f)$  is the cross-power-spectral density function.

## 4. RELATIONSHIP BETWEEN AMPLIFICATION AND SITE PARAMETERS

We examine the relationship between site amplification ( $S/B'$ ) and site variables describing the depth and stiffness of the deposit. As a commonly-used index parameter for the shear-wave velocity profile, we use the average shear-wave velocity in the uppermost 30 m  $V_{S30}$ .

# All KiK-net stations (1998-2009)

S/B' (horizontal components) as a function of  $V_{s30}$

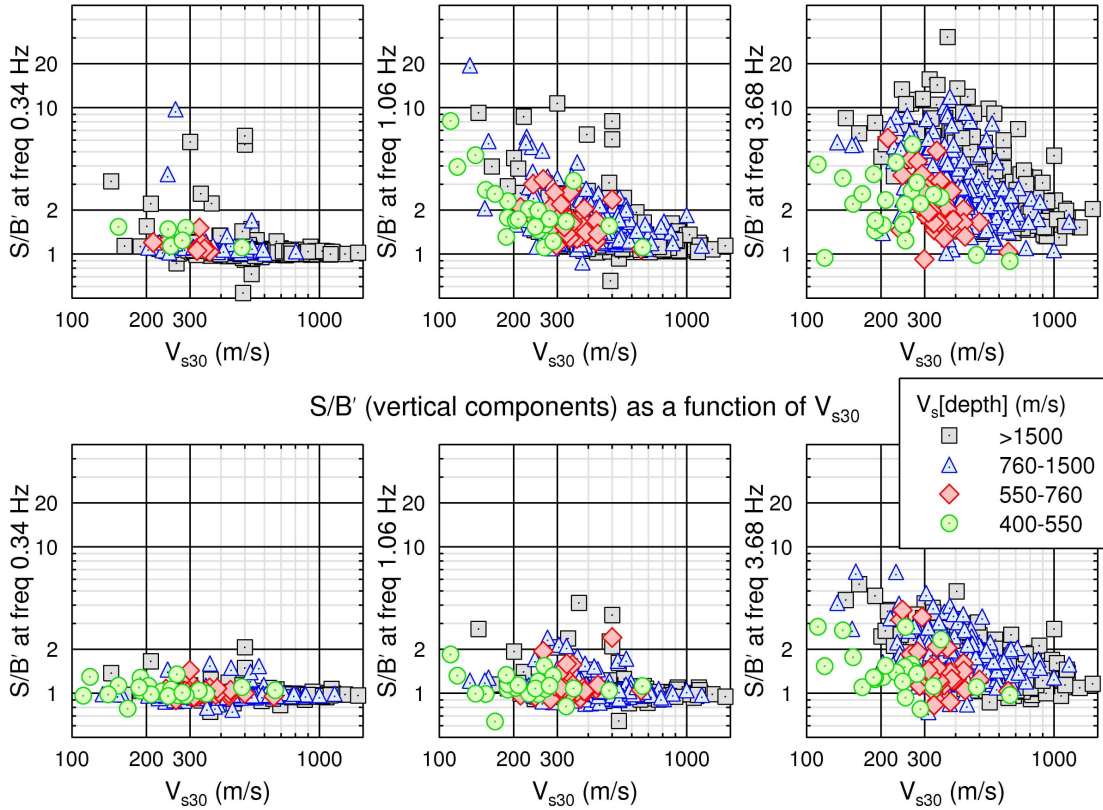


**Figure 1.** Amplification ( $S/B'$ ) for the KiK-net stations relative to  $V_{s30}$ . Sites are categorized into four groups based on their  $V_s[\text{depth}]$  which is the shear-wave velocity at the depth of installation.

Figure 1 explores the relationship between site amplification and  $V_{s30}$ , considering all KiK-net data. We see some evidence for greater amplification, for the same  $V_{s30}$ , if  $V_s[\text{depth}] \geq 760$  m/s, due to impedance effects. But the amplification for the data in the range 760-1500 m/s appears to be about the same as that for  $V_s[\text{depth}] > 1500$  m/s. Therefore, the  $S/B'$  ratio data for  $V_s[\text{depth}] \geq 760$  m/s are used to characterize the overall site amplification. We perform a simple least-squares regression to determine the amplification for each frequency:

$$\log(S/B') = m \cdot \log(V_{s30}/V_{ref}) + b \quad (3)$$

where  $V_{ref} = 760$  m/s. The regression coefficients are tabulated in Table 1 for several representative frequencies.

**Table 1.** Coefficients for site correction factors, horizontal component

Frequency (Hz)	Tohoku		All KiK-net	
	$m$	$b$	$m$	$b$
0.52	-0.248	0.027	-0.211	0.023
0.99	-0.518	0.063	-0.491	0.055
1.90	-0.748	0.157	-0.768	0.148
4.55	-0.622	0.338	-0.724	0.357
8.75	-0.076	0.447	-0.205	0.495
10.88	0.057	0.438	-0.014	0.490

Another important site parameter, in addition to site stiffness/shear-wave velocity, is the fundamental resonance frequency ( $f_0$ ). The fundamental frequency depends on both layer depth and stiffness, and may carry information on deeper part of the soil column, in comparison to  $V_{S30}$  which considers only the top 30 m. The fundamental frequency is obtained for the KiK-net data using the peak of the horizontal-to-vertical (H/V) spectral ratios of the recorded strong motions at the sites (Lermo and Chávez-García, 1993).

The fundamental frequency  $f_0$  is related to the depth-to-bedrock (i.e.  $f_0 = V_S/4HB$ ). Depth-to-bedrock (HB), defined by the depth of a layer with  $V_S = 760$  m/s, or to a significant impedance contrast between surface soil deposits and material with  $V_S = 760$  m/s, is obtained for each site from the velocity profile. Figure 2 plots  $f_0$  as a function of  $V_{S30}$ , respectively. Results indicate that  $V_{S30}$  is a good proxy to estimate the natural frequency of a site. Furthermore, the fundamental frequency inferred from the H/V ratios matches well with that derived from the theoretical relation ( $f_0 = V_S/4HB$ ).

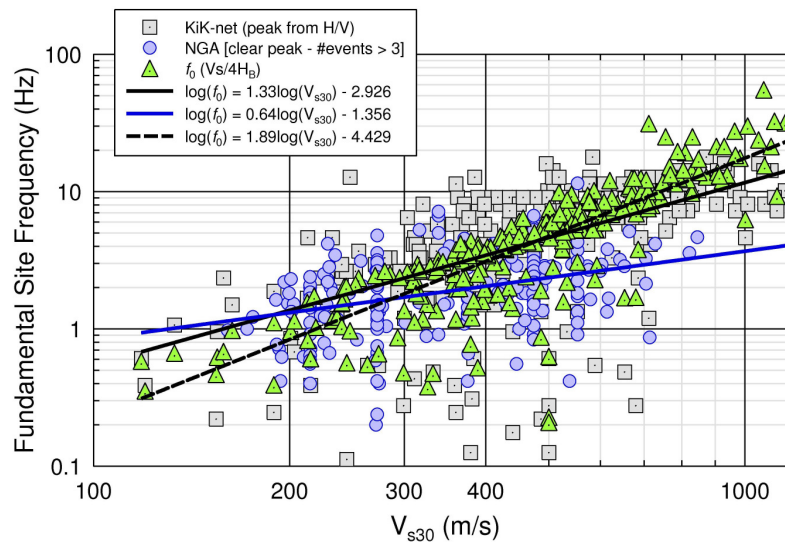


**Figure 2.** Fundamental site frequency ( $f_0$ ) as a function of  $V_{S30}$ . Lines are the best linear fit to  $f_0$  as a function of  $V_{S30}$  for each dataset.

To check if the  $V_{S30}$ - $f_0$  correlation is valid in other tectonic regions, we use the 2005 Pacific Earthquake Engineering Research (PEER) Center global ground motion database, which was used for the development of the 2008 NGA-West models (shallow events in active tectonic regions). We calculate the H/V ratios for all sites in the PEER-NGA database and pick the fundamental frequencies, considering just those stations that show a clear single peak and that recorded at least 3 events. The slope of the  $V_{S30}$ - $f_0$  relation ( $0.64 \pm 0.10$ ) is less than that for Japan ( $1.33 \pm 0.12$ ). The lower values of  $f_0$  for the NGA data indicate deeper bedrock, for the same  $V_{S30}$ , in most regions that comprise the NGA database.

Figure 3 plots the fundamental site frequency as a function of depth-to-bedrock, which is interrelated to  $V_{S30}$ . We also show in Fig. 3 the corresponding relationship for the PEER-NGA strong motion dataset; for the PEER-NGA data, the “depth to bedrock” is assumed to be the depth to  $V_S = 1.0$  km/s (Z1.0), as it is the closest proxy to our selected  $V_S = 760$  m/s. The Japan and PEER-NGA data show similar trends, but there is a higher intercept for the PEER-NGA data, probably because they are referenced to stiffer, deeper bedrock. We also show the estimated Z1.0 values from the velocity profiles of KiK-net stations in Fig. 3.

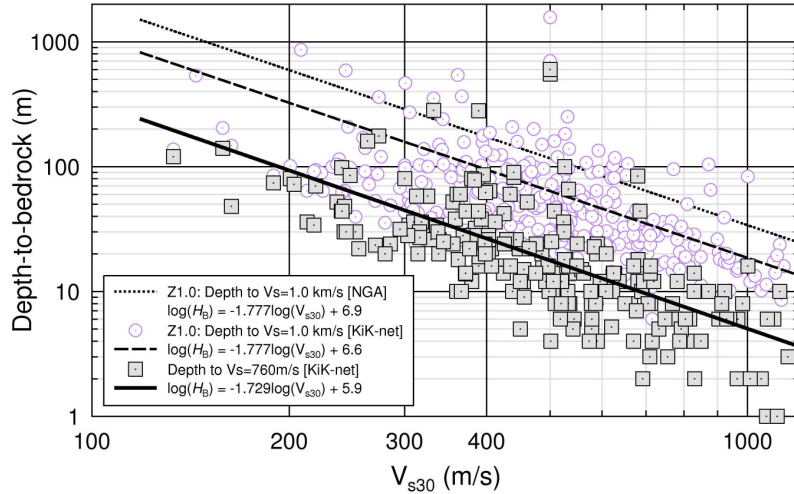


**Figure 3.** Depth-to-bedrock as a function of  $V_{S30}$ . The dotted line is the best fit to the Z1.0 from the NGA database. The dashed line is the estimated model for predicting Z1.0 in Japan.

## 5. USING H/V AS AN EXTRA PARAMETER FOR SITE AMPLIFICATION FUNCTION

The H/V spectral ratio has been widely used to provide a preliminary estimate of site amplification (Nakamura, 1989). We explore the use of H/V as an amplification function for the KiK-net data. This will be useful for other applications where H/V is known but borehole data are not available to constrain site amplification. We performed a linear regression using:

$$\log(Y) = a_1 \cdot \log(V_{S30}) + a_2 \cdot \log(f_0) + a_3 \quad (4)$$

where  $Y$  is the ratio of the site amplification ( $S/B'$ ) to the average of H/V. By using H/V and  $V_{S30}$  with Eqn. 4, we obtain a good match to the observed site transfer functions for the whole range of frequencies (Fig. 4). The advantage of this method could be significant for assessing the site effects by using a single station or in an area where a rock reference site cannot be found.

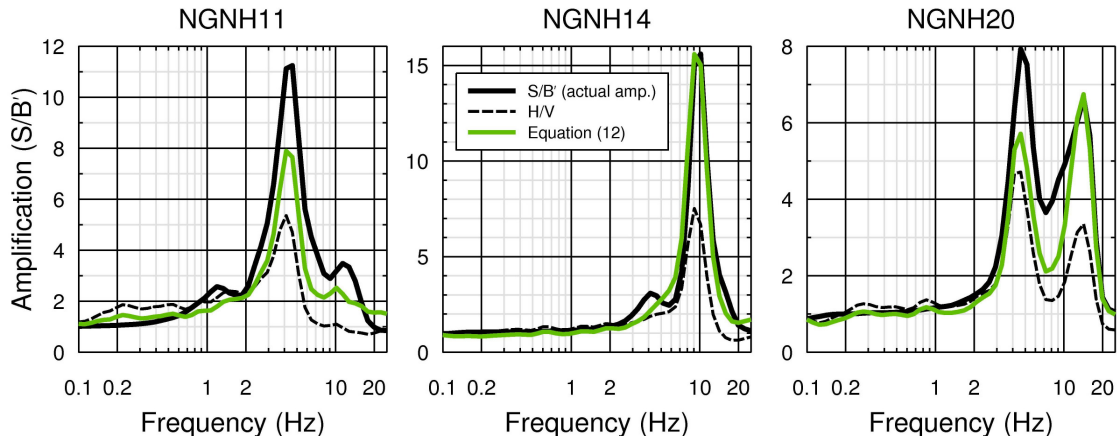


**Figure 4.** Comparison of  $S/B'$  ratios using cross-spectral ratios (solid black line) for NGNH11, NGNH14, and NGNH20 with mean H/V ratios (dashed black line). Transfer functions are overlaid by prediction model using  $V_{S30}$  and  $f_0$  as predictor parameters and adding H/V as an extra parameter (green line).

## 6. NON-LINEAR SITE AMPLIFICATION

Under strong shaking, soil may exhibit nonlinear and hysteretic behavior, with the effective modulus  $G$  decreasing at high strain (Beresnev and Wen, 1996). As a consequence, nonlinearity will result in a shift of the resonance frequency to lower values, and the reduction in amplification, as the amplitude of motions increases (Silva, 1986).

Figure 5 shows the nonlinear behavior of a site subjected to strong ground shaking (peak ground acceleration (PGA)  $\sim 530 \text{ cm/s}^2$ ). The spectral ratio for MYGH04 is compared for the strongest part of the signal and the coda-window, noting that the shaking during the coda is a representative of weak-motion (Chin and Aki, 1991).

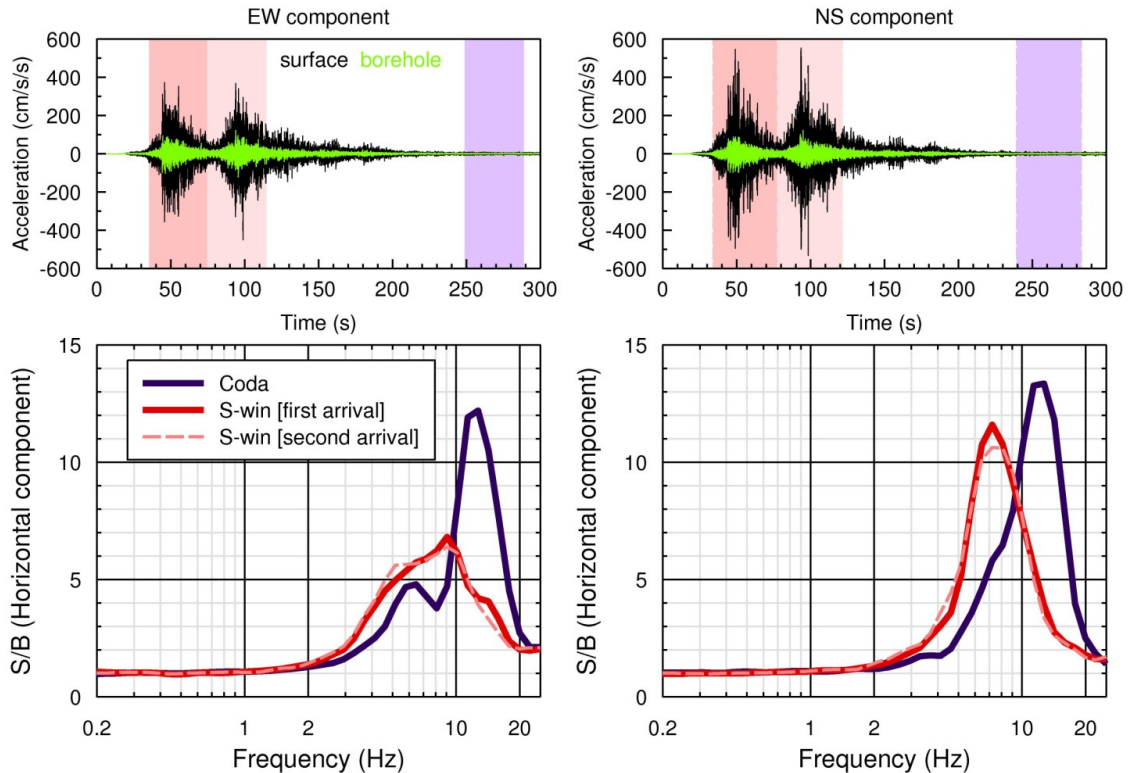


**Figure 5.** Amplification of EW and NS components at MYGH04 for the S-window of the first arrival (thick solid red), S-window of the second arrivals (dashed light red), and coda-window (blue).

From Fig. 5, a clear shift of the peak amplitude frequency to lower frequencies during the strong shaking portion of the record can be seen. Also, the amplitudes are reduced for the S-window spectral ratios in comparison with the coda-window spectral ratios.

The Short-Time Fourier Transform (STFT) analysis (Wu et al., 2010) is carried out to identify the PGA threshold of nonlinearity using both surface and borehole time series for each station. A decrease of fundamental frequency and amplitude due to the nonlinear behavior of a site can be detected within strong part of the signal, relative to the coda window and background noise (Fig. 6).

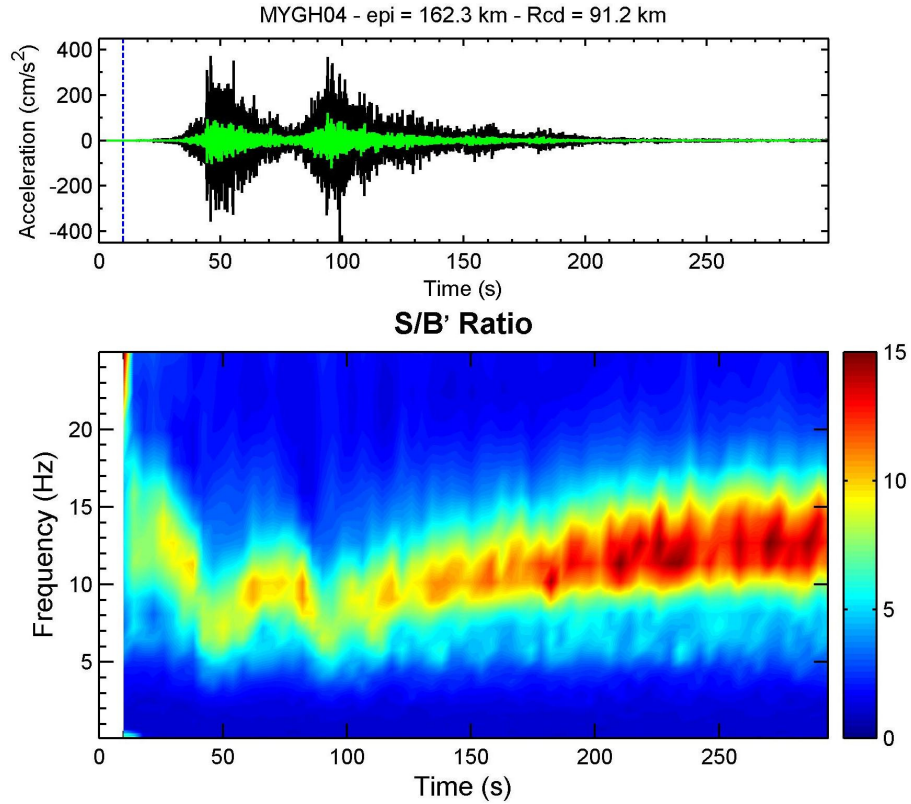


**Figure 6.** Temporal evolution of S/B for the MYGH04 station.

We calculate the average of spectral ratios at each station over all events ( $A_{\text{ref}}$ ) and the frequency of that peak ( $f_{\text{ref}}$ ). The same procedure is repeated for calculating spectral ratios at the same sites for the Tohoku earthquake. In this case, the maximum amplitude (for the mainshock) is called  $A_{\text{MS}}$  and the fundamental frequency is called  $f_{\text{MS}}$ . We consider stations that show a clear, single peak in the H/V at the surface alone. In total, 225 out of 475 stations passed these criteria and among them only 42 stations showed nonlinear behavior (shifting of the fundamental frequency to lower frequencies, and a decrease in amplitude). To quantify the nonlinear behavior at these 42 stations, in Fig. 7 we plot the ratio  $A_{\text{MS}}/A_{\text{ref}}$  and  $f_{\text{MS}}/f_{\text{ref}}$  as a function of  $\text{PGA}_{\text{ref}}$ , which is the predicted median PGA by the Tohoku regression Eqn. 5 (derived below), for  $V_{\text{S}30} = 760$  m/s (reference). The plots show that there is a weak but steady trend indicating nonlinear behavior, even from low amplitude, for all soil types. The slope and standard error of the best fitted line for  $A_{\text{MS}}/A_{\text{ref}}$  is  $-0.0018 \pm 0.0014$ . For the  $f_{\text{MS}}/f_{\text{ref}}$  ratio, the slope is  $-0.0028 \pm 0.0009$ . The behavior for stations that did not show non-linear behavior is plotted in the background on these figures (and not used in fitting the lines). If all data are used to fit the lines giving  $A_{\text{MS}}/A_{\text{ref}}$  and  $f_{\text{MS}}/f_{\text{ref}}$  as a function of  $\text{PGA}_{\text{ref}}$ , the obtained slope is not significantly different from zero. This illustrates that nonlinearity is not pervasive, at least for these levels of  $\text{PGA}_{\text{ref}}$ . It should be kept in mind that even though the input  $\text{PGA}_{\text{ref}}$  levels are relatively modest ( $<10\%$ g), the PGA on the surface often exceeds  $50\%$ g due to the large high-frequency amplifications (factors of 5 or more) at many of the sites.

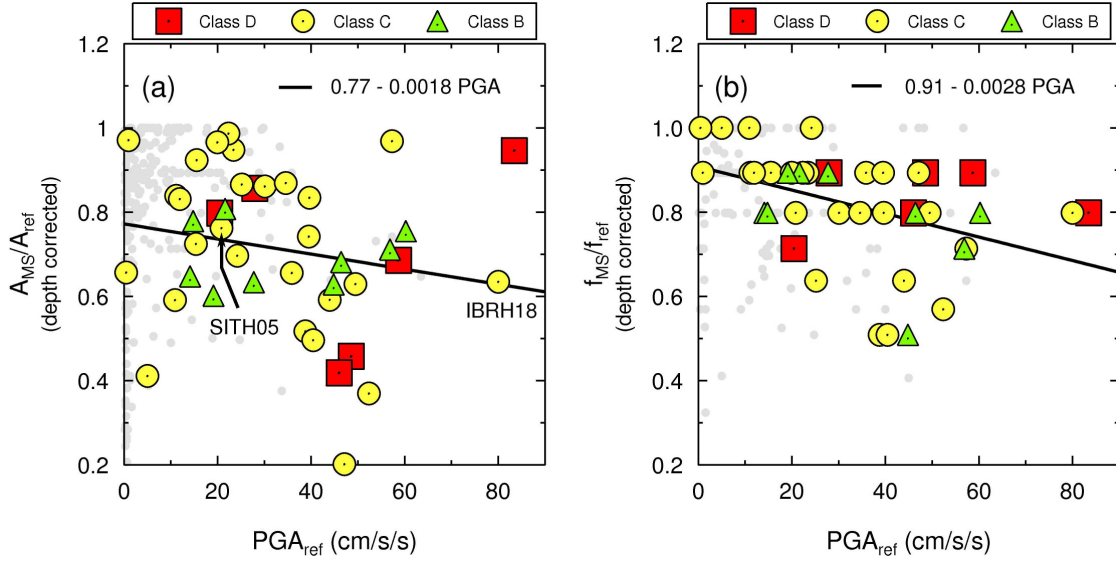


**Figure 7.** Nonlinearity symptoms at the KiK-net stations, such as a decrease in the predominant frequency and/or amplification amplitude as a function of  $PGA_{ref}$  (predicted for  $V_{S30} = 760$  m/s). Colored symbols used to fit non-linear trend line (for stations showing evidence of nonlinearity). Other stations (linear) shown by gray dots.

We conclude that nonlinearity, though present in some cases, was not a pervasive phenomenon during the Tohoku event for the KiK-net sites; only a small fraction of sites show amplitude and frequency content that are shifted significantly. However, it should be mentioned that there are many cases for liquefaction-related damage during the Tohoku earthquake.

## 7. OVERALL CHARACTERISTICS OF TOHOKU GROUND MOTIONS

Having evaluated site amplification for the Tohoku motions, we can now characterize the Tohoku ground motions with site effects removed. We fit the site-corrected Tohoku motions using:

$$\log(PSA) + \log(R_{eff}) - site_{factor} = c_0 + c_1 \cdot F \cdot R + c_2 \cdot B \cdot R \quad (5)$$

where  $R_{eff} = \sqrt{R_{cd}^2 + 10^2}$  and  $R_{cd}$  is the closest distance to the fault rupture surface. For stations in the forearc region,  $F = 1$  and  $B = 0$ , while for backarc stations,  $F = 0$  and  $B = 1$  (Ghofrani and Atkinson, 2011). The  $site_{factor}$  is calculated using coefficients in Table 1. The regression coefficients are given for pseudo-spectral acceleration (PSA) in Table 2.

**Table 2.** Regression coefficients for PSA (geometric mean of horizontal components)

Frequency (Hz)	PSA (cm/s <sup>2</sup> )		
	$c_0$	$c_1$	$c_2$
0.52	3.96	-0.0005	-0.0013
0.99	4.19	-0.0009	-0.0019
1.90	4.30	-0.0011	-0.0024
4.55	4.33	-0.0013	-0.0028
8.75	4.28	-0.0010	-0.0028
10.88	4.23	-0.0009	-0.0027

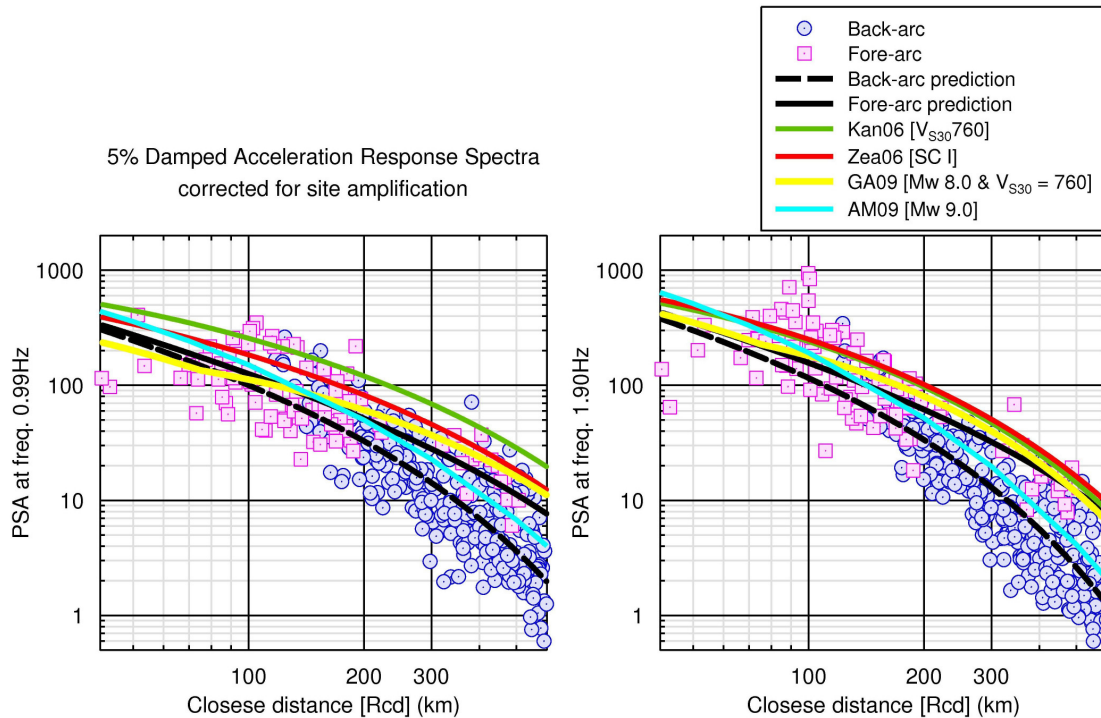


**Figure 8.** Comparing event-specific prediction equation for the site corrected Tohoku ground-motions (B/C) with other GMPEs (Kan06 = Kanno et al. [2006]; Zea06 = Zhao et al. [2006]; AM09 = Atkinson and Macias [2009]; and GA09 = Goda and Atkinson [2009]) at four frequencies.

A comparison between the event-specific Tohoku prediction equation and motions predicted by regional GMPEs for Japan is shown in Figure 8. The observed PSA values are corrected for site amplification using coefficients from Table 1, before comparison with GMPEs for a reference condition of B/C. Empirical GMPEs, including those by Zhao et al. (2006), Kanno et al. (2006) and Goda and Atkinson (2009), are not constrained by data for  $M > 8.5$ , so we have chosen to plot these relations for  $M = 8.5$  to avoid over-extrapolating amplitudes at larger magnitudes. The Atkinson and Macias (2009) GMPE is based on stochastic finite-fault simulations, and may be fairly evaluated at  $M = 9.0$ . The Zae06 and Kan06 GMPEs are over-predicting Tohoku ground motions at 1.0 Hz, while AM09 is similar to the new equation for the back-arc stations. It is clear from Fig. 8 that the attenuation (slope and curvature) of single Q-factor GMPEs – especially in subduction zones – is controlled mostly by the backarc stations.

## 8. CONCLUSIONS

The 2011 M9.0 Tohoku earthquake has provided important new quantitative information on site response that is invaluable in refining strong ground motion studies, seismic hazard analysis, and mitigation efforts. The conclusions that are drawn from the analyses are:

- The site amplifications are much greater than those indicated by standard building code factors based on NEHRP site class (factors of 4 to 8 at  $f > 2$  Hz).
- Empirical relationships may be used to predict site amplification using H/V, VS30, and  $f_0$ .
- Nonlinear site response was not pervasive during the 2011 M9.0 Tohoku earthquake.
- Generic GMPEs developed for subduction regions appear to under-estimate the Tohoku motions if soil amplification effects are not removed. However, once site effects are taken into account the agreement is more reasonable.

## ACKNOWLEDGEMENTS

Ground-motion data and site information were obtained from KiK-NET at <http://www.kyoshin.bosai.go.jp>, the NIED strong-motion seismograph networks.

## REFERENCES

- Atkinson, G. M. and Casey, R. (2003). A comparison of ground motions from the 2001 M6.8 in-slab earthquakes in Cascadia and Japan. *Bull Seism Soc Am.* **93**: **4**, 1823-1831.
- Atkinson, G. M. and Macias, M. (2009). Predicted ground motions for great interface earthquakes in the Cascadia subduction zone. *Bull Seism Soc Am.* **99**: **3**, 1552-1578.
- Beresnev, I. A. and Wen, K-L (1996). The accuracy of soil response estimates using soil-to-rock spectral ratios. *Bull Seism Soc Am.* **86**: **2**, 519-523.
- Borcherdt, R. D. (1970). Effects of local geology on ground motion near San Francisco Bay. *Bull Seism Soc Am.* **60**: **1**, 29-61.
- Chin, B. H. and Aki, K. (1991). Simultaneous study of the source, path, and site effects on strong ground motion during the 1989 Loma Prieta earthquake: a preliminary result on pervasive nonlinear site effects. *Bull Seism Soc Am.* **81**: **5**, 1859-1884.
- Field, E. H. and Jacob, K. H. (1995). A comparison and test of various site-response estimation techniques, including three that are not reference site dependent. *Bull Seism Soc Am.* **85**: **4**, 1127-1143.
- Fukushima Y, Bonilla LF, Scotti O, Douglas J (2007) Site classification using horizontal-to-vertical response spectral ratios and its impact when deriving empirical ground motion prediction equations. *Journal of Earthquake Engineering.* **11**: **5**, 712-724.
- Ghofrani, H. and Atkinson, G. M. (2011). Fore-arc versus back-arc attenuation of earthquake ground motion. *Bull Seism Soc Am.* **101**: **6**, 3032-3045.
- Goda, K. and Atkinson, G. M. (2009). Probabilistic characterization of spatially-correlated response spectra for earthquakes in Japan. *Bull Seism Soc Am.* **99**: **5**, 3003-3020.
- Kanno, T., Narita, A., Morikawa, N., Fujiwara, H. and Fukushima, Y. (2006). A new attenuation relation for strong ground motion in Japan based on recorded data. *Bull Seism Soc Am.* **96**: **3**, 879-897.
- Lermo, J. and Chávez-García, F. J. (1993). Site effects evaluation using spectral ratios with only one station. *Bull Seism Soc Am.* **83**: **5**, 1574 - 1594.
- Nakamura, Y. (1989). A Method for Dynamic Characteristics Estimation of Subsurface using Microtremor on the ground surface. *Railway Technical Research Institute, Quarterly Reports.* **30**: **1**, 25-33.
- Silva, W. J. (1986). Soil response to earthquake ground motion, report prepared for Electric Power Research Institute, *EPRI Research Project RP 2556-07.*
- Steidl, J. H., Tumarkin, A. G. and Archuleta, R. J. (1996). What is a reference site? *Bull Seism Soc Am.* **86**: **6**, 1733-1748.
- Theodulidis, N. and Bard, P-Y (1995). Horizontal to vertical spectral ratio and geological conditions: an analysis of strong motion data from Greece and Taiwan (SMART-I). *Soil Dyn Earthquake Eng.* **14**: **3**, 177- 197.
- Wu, C., Peng, Z. and Ben-Zion, Y. (2010). Refined thresholds for nonlinear ground motion and temporal changes of site response associated with medium size earthquakes. *Geophys J Int.* **182**: **3**, 1567-1576.
- Zhao, J. X., Zhang, J., Asano, A., Ohno, Y., Oouchi, T., Takahashi, T., Ogawa, H., Irikura, K., Thio, H. K., Somerville, P. G., Fukushima, Y. and Fukushima, Y. (2006). Attenuation relations of strong ground motion in Japan using site classification based on predominant period. *Bull Seism Soc Am.* **96**: **3**, 898-913.